Eur. Phys. J. C 17, 413–421 (2000)
Digital Object Identifier (DOI) 10.1007/s100520000489

THE EUROPEAN PHYSICAL JOURNAL C

NLL Monte-Carlo approach in 1 or 2 jets photoproduction*

P. Aurenche[1], L. Bourhis[3], M. Fontannaz[2], J. Ph. Guillet[1]

[1] Laboratoire de Physique Théorique LAPTH[a], B.P. 110, 74941 Annecy-le-Vieux Cedex, France
[2] Laboratoire de Physique Théorique[b], Université de Paris XI, bâtiment 210, 91405 Orsay Cedex, France
[3] Department of Theoretical Physics, South Road, Durham City DH1 3LE, UK

Received: 1 June 2000 / Revised version: 19 July 2000 /
Published online: 25 September 2000 – © Springer-Verlag 2000

Abstract. We present a method for calculating the photoproduction of jets at HERA based on Next to Leading Logarithm QCD calculations. It is implemented in a Monte-Carlo generator which allows us to easily compute any infra-red safe cross sections for 1 or 2 jet observables using various jet reconstruction algorithms. We focus on the possibility of extracting the gluon contents of the photon and of the proton from present and future H1 and ZEUS data.

1 Introduction

Electron-proton scattering at HERA is dominated by the exchange of a quasi-real photon and a fraction of γ-p collisions leads to the production of high p_T jets. Therefore these processes can be predicted by perturbative QCD and they can be used to investigate the structure of the photon in a way complementary to the study of the deep inelastic scattering e-γ. In the latter case, one can measure directly the quark density inside the photon whereas the gluon density is constrained by the evolution equation. On the contrary, in photoproduction, one can probe directly the gluon contents of the photon.

Leading Logarithm (LL) results have been available for a long time, but they are plagued by sizeable uncertainties coming from the dependence on unphysical scales. Therefore, Next to Leading Logarithm (NLL) calculations are essential to describe the photoproduction of jets. To reach this goal, we have adapted a method developped previously to deal with the production of two high-p_T hadrons in hadron collisions [1]. We apply it to build a Monte-Carlo generator which is able to produce a set of partonic events on which one can apply any jet reconstruction algorithm to produce a set of jet events. With the latter we can easily compute any infrared safe cross sections. This technique gives a lot of flexibility to the study of various jet algorithms and observables.

In particular we will apply it to the study of two jet observables in which the distribution function variables are well constrained by kinematics. This allows us to disentangle the distribution functions from the hard subprocess more easily, because less convolutions are involved in the calculation of the cross sections. Some results obtained with this approach have already been reported in [2].

The paper is organised as follows. The theoretical framework is described in Sect. 2. We also compare our approach with those of other authors. In Sect. 3 we present some applications of our work to 1-jet cross sections and we compare our results with those already obtained with an analytical approach. Section 4 is devoted to the study of 2-jet observables. We will examine whether it is possible to accurately measure the distribution functions of the gluon in the photon and in the proton. In Sect. 5 we study recent H1 and ZEUS data and the constraints they put on the gluon distributions. The conclusions are in Sect. 6.

2 Description of the method

To calculate cross sections and isolate collinear and infrared singularities, we used a "phase space slicing method". We start from the $2 \to 3$ partonic squared matrix elements and virtual corrections evaluated by Ellis and Sexton [3]. Collinear and infra-red singularities lead to poles in $1/\epsilon$ and $1/\epsilon^2$ when using dimensional regularisation. For a generic real process $1 + 2 \to 3 + 4 + 5$, at least two partons have high transverse energy E_T (3 and 4) and only one can be soft (5). In order to extract the singularities, we cut the phase space in several parts: part I where E_{T5} is less than a given scale p_{Tm} and part II where $E_{T5} > p_{Tm}$. Part II is divided in three parts: IIa (resp. IIb) where parton 5 is within a cone around parton 3 (resp. 4) called C_3 (resp. C_4), IIc where parton 5 is outside C_3 and C_4. Parton 5 is in C_i if $((\phi_5-\phi_i)^2+(\eta_5-\eta_i)^2)^{\frac{1}{2}} < R_c$. Here $\eta = -\log\tan(\theta/2)$ is the pseudo-rapidity and ϕ is the azimuthal angle. Part I contains infra-red singularities and

* This work was supported in part by the EU Fourth Framework Programme "Training and Mobility of Researchers", Network "Quantum Chromodynamics and the Deep Structure of Elementary Particles", contract FMRX-CT98-0194 (DG 12 - MIHT)

[a] URA 14-36 du CNRS, associée à l'Université de Savoie
[b] Unité Mixte de Recherche CNRS - UMR 8627

collinear singularities in the initial state and parts IIa and IIb contain collinear singularities in the final state whereas part IIc is finite.

The contributions of regions I, IIa and IIb are calculated analytically and the infra-red singularities are cancelled by the corresponding ones in the virtual terms. Initial collinear singularities are factorised in the parton distributions and the final collinear singularities disappear when integrating on the relative momentum between parton 5 and the parton with which it is collinear due to energy momentum sum rules.

The finite parts remaining after the cancellation of singularities have been analytically computed using Maple [4]. Large logarithms $\log p_{Tm}$, $\log^2 p_{Tm}$ and $\log R_c$ appear in the collinear and infrared contributions. They are cancelled by similar terms from part IIc so that the total cross section is independent of these unphysical cuts. It should be noted that we have kept only the logarithmic terms in the calculation of contributions I, IIa and IIb, neglecting terms of order $\mathcal{O}(p_{Tm}\log p_{Tm})$, $\mathcal{O}(R_c^2\log p_{Tm})$, and less singular terms.

Using the Monte-Carlo package BASES [5], our program generates quasi $2 \to 2$ events corresponding to collinear, Born and virtual contributions (we take $p_{Tm} \ll E_{T_{3,4}}^{min}$ and $R_c \ll 1$) and $2 \to 3$ events corresponding to part IIc. For the latter, a jet reconstruction algorithm is applied. Finally, these events are histogrammed [6] in order to give any cross sections we are interested in. We have checked that the cross sections do not depend on the unphysical cuts p_{Tm} and R_c in the region where $0.005 < p_{Tm} < 0.1$ and $0.01 < R_c < 0.1$. From a numerical point of view, the compensation between this cut dependence arises mainly between positive real contribution of part IIc and negative contributions of part I, IIa, IIb and virtual corrections; we need to generate a sufficient number of events in order to obtain a small error after the compensation. We take the greatest possible values for the cuts p_{Tm} and R_c (i.e. $p_{Tm} = 0.1\ GeV$ and $R_c = 0.1$) in order to lower the size of this compensation which is then typically of the order of 1 for 5.

This approach is applied to the direct and resolved (proportional to the photon distribution functions) parts of the cross section. However these contributions depend on the convention adopted in the subtraction of the collinear singularities. Unless explicitly specified, we use the $\overline{MS}$ factorization and renormalization schemes.

Several authors have used similar approaches in the calculation of jet-photoproduction cross sections. Harris and Owens [7] also built an event generator; but their phase slicing is based on cuts put on E_5 (in the parton CM) and on the Mandelstam variables of the subprocess which control the collinear divergences. Klasen and Kramer [8] introduced a single invariant cut on the Mandelstam variables. On the other hand Frixione and Ridolfi [9] made their calculations with the subtraction method [10]. We made several numerical comparisons with the results of Klasen and Kramer, and found a good agreement.

Finally let us note that it is very convenient to use variables E_T, η and ϕ to define regions of the phase space in which we perform analytical calculations. Indeed these are the variables commonly used by experimentalists to define jets and cuts in their phase space. If p_{T_m} and R_c are smaller than respectively the lower bound of the transverse momenta and the width of jets, we never integrate (thus defining an inclusive measurement) in a phase space region in which the experimentalists perform an exclusive measurement. Since these experimental bounds are much larger than the domain in which our neglecting non logarithmic terms is valid this is in fact not a constraint at all. On the contrary with the invariant cut method, this can only be achieved with very small cuts.

3 Single jets

In this section we present some numerical results for one-jet cross sections in order to compare our predictions with those obtained in a preceding paper [11]. Our inputs are the following. At the HERA collider ($\sqrt{s} = 300$ GeV), electrons produce photons with small virtuality Q^2. We use the kinematical conditions of the ZEUS collaboration [12]: $Q^2_{max} = 1\ GeV^2$ and $0.2 < y < 0.85$ where $y = E_\gamma/E_e$. The spectrum of the quasi-real photon is approximated by the We acker-Williams formula.

$$F_e^\gamma(y) = \frac{\alpha}{2\pi}\left\{\frac{1+(1-y)^2}{y}\ \log\ \frac{Q^2_{max}(1-y)}{m_e^2\ y^2} - \frac{2(1-y)}{y}\right\}. \quad (1)$$

For the proton distributions we take the CTEQ4M parametrization [13] and for the photon distributions the GRV parametrization [14] transformed to the $\overline{MS}$ scheme. We use five flavours, $\Lambda^{(4)}_{\overline{MS}} = 296$ MeV, a renormalization scale μ and a factorization scale M equal to the transverse energy E_T of the jet. For all our calculations, we use for $\alpha_s(\mu)$ an exact solution of the two-loop renormalization group equation, and not an expansion in $\log\frac{\mu}{\Lambda}$. The cross sections are higher by some 2.5% when the exact $\alpha_s(\mu)$ is used with $\mu \sim 15$ GeV.

Here we present results only for the resolved contribution. Jets are defined with the k_T-algorithm [15]. We compare our results with those of a previous analytical calculation [11], for the transverse momentum distribution in Fig. 1a and for the rapidity distribution in Fig. 1b. We can see that the agreement is quite good between these two sets of results. Similar comparisons hold for the direct part.

We do not pursue the study of 1-jet cross sections, because they do not constrain the parton distributions as well as the 2-jet cross sections do; the latter offer more kinematical possibilities of control of the x-variable of these distributions.

4 Dijets cross sections and the photon structure function

In this section we study the dijet cross sections and put the emphasis on variables and cross sections which give access

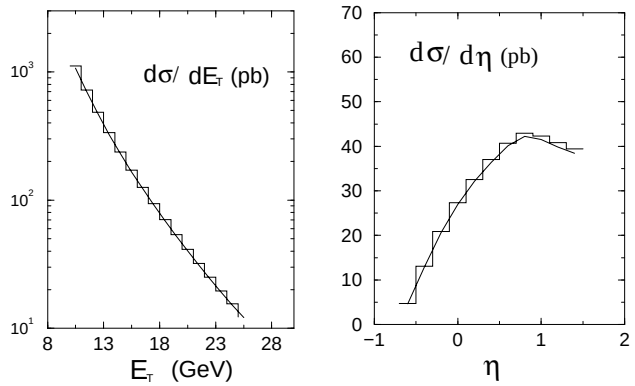

Fig. 1a,b. **a** Single jet resolved cross section $d\sigma/dE_T$ integrated in the rapidity range $.5 \leq \eta \leq 1.5$ (histogram) and compared to the analytical result of [11]. **b** $d\sigma/d\eta$ for the resolved contribution with 20 GeV $< E_T <$ 21 GeV

to the gluon distribution functions. Comparison between data and theory is postponed to Sect. 5. The dijet cross section, as a function of the transverse energy E_{T3} and the jet rapidities η_3 and η_4, is given by a product if the subprocess is a $2 \to 2$ reaction (LL approximation)

$$\frac{d\sigma}{dE_{T3}^2 d\eta_3 d\eta_4} = \sum_{a,b,c,d} x_e\ F_e^a(x_e, M)\ x_p\ F_p^b(x_p, M) \times \frac{d\sigma_{ab\to cd}(\mu)}{dt} \quad , \tag{2}$$

$d\sigma/dt$ is the $a + b \to c + d$ cross section, and $F_e^a(F_p^b)$ the parton distributions in the electron (proton) ($x_p = E_{T3}(e^{\eta_3} + e^{\eta_4})/2E_p$ and $x_e = E_{T3}(e^{-\eta_3} + e^{-\eta_4})/2E_e$); M is the factorization scale and μ the renormalization scale. The direct contribution corresponds to $a = \gamma$ and F_e^γ is the Weizsäcker-Williams formula (1). In the resolved case, F_e^a is given by a convolution of F_e^γ with the parton distribution in the photon

$$F_e^a(x_e, M) = \int_0^1 dy\ dx_\gamma\ F_e^\gamma(y)\ F_\gamma^a(x_\gamma, M) \times \delta(x_\gamma y - x_e) \quad . \tag{3}$$

If the photon energy $E_\gamma = yE_e$ is known (for instance by tagging the outgoing electron), we can measure x_γ and define the observable

$$\frac{d\sigma}{dx_\gamma} = \sum_{a,b,c,d} x_\gamma\ F_\gamma^a(x_\gamma, M) \int_0^1 dy\ dE_{T3}^2 d\eta_3 d\eta_4\ \delta \times \left(x_\gamma - \frac{E_{T3}\left(e^{-\eta 3} + e^{-\eta_4}\right)}{E_\gamma} \right) \times F_e^\gamma(y)\ x_p\ F_p^b(x_p, M) \frac{d\sigma}{dt} \ . \tag{4}$$

Thus the dijet cross section written as a function of x_γ is proportional to the parton distribution in the photon $F_\gamma^a(x_\gamma)$. One observes that the direct contribution, with $F_\gamma^a = \delta_{\gamma_a}\delta(1 - x_\gamma)$, leads to a peak in the cross section at $x_\gamma = 1$.

NLL QCD corrections to the LL expression (4) blur its simple kinematics. There are contributions with three jets in the final state, and we can no longer fix $x_\gamma = \sum_{i=3}^{5} \frac{E_{Ti} e^{-\eta_i}}{2E_\gamma}$, because the third jet is not observed. However we can follow the strategy of the ZEUS collaboration [16] which defines the variable (jets 3 and 4 are the jets with the highest transverse energies)

$$x_\gamma^{obs} = \frac{(E_{T3} e^{-\eta_3} + E_{T4} e^{-\eta_4})}{2E_\gamma} \tag{5}$$

and observe the dijet cross section $d\sigma/dx_\gamma^{obs}$. However this definition of x_γ^{obs} may lead to infrared sensitive cross sections. Indeed fixing E_{T3} and E_{T4} strongly constrains the available phase space of the unobserved partons (for instance parton 5 in Sect. 2) and forbids a complete compensation between real and virtual NLL corrections. This results in cross sections containing, for instance, terms proportional to $\log\left(1 - \left(E_{T4}^{min}/E_{T3}\right)^2\right)$ after an integration over E_{T4} from a lower bound E_{T4}^{min} (smaller than E_{T3}) has been performed. The cross section is not defined at $E_{T3} = E_{T4}^{min}$, although it is integrable. Therefore the variable x_γ^{obs} defined in (5) should only be used with cross sections integrated over E_{T3} and E_{T4}; moreover the integration range of E_{T3} and E_{T4} should not have the same bounds. A discussion of this condition may be found in [9].

For these reasons, we prefer the variable

$$x_\gamma^{LL} = \frac{E_{T3}\,(e^{-\eta_3} + e^{-\eta_4})}{2E_\gamma} \tag{6}$$

which depends on the transverse energy of only one jet. It can be associated with cross sections in which the energy of the second jet is not measured. One observes that x_γ^{LL} may take values larger than 1.0.

One must also observe that the cross sections $d\sigma/dx_\gamma^{LL}$ or $d\sigma/dx_\gamma^{obs}$ are singular when x_γ^{LL} or x_γ^{obs} approaches 1. Indeed we have the condition

$$1 \geq \frac{E_{T3}\ e^{-\eta_3} + E_{T4}\ e^{-\eta 4} + E_{T5}\ e^{-\eta_5}}{2E_\gamma}$$

(the sign = corresponds to the direct case), which means

$$1 - x_\gamma^{obs} \geq \frac{E_{T5}\ e^{-\eta_5}}{2E_\gamma} \quad . \tag{7}$$

When x_γ^{obs} goes to 1, the phase space of parton 5 is severely restricted. This results in $\log(1 - x_\gamma^{obs})$ terms generated by the NLL corrections. We obtain a similar result with $x_\gamma^{LL} \to 1$, although the phase space of parton 5 is less severely constrained than by condition (7). Therefore we expect a smoother behaviour of $d\sigma/dx_\gamma^{LL}$. This point can be verified in Fig. 2 in which we display $d\sigma/dx_\gamma^{obs}$ and $d\sigma/dx_\gamma^{LL}$ for the direct term. Besides the region very close

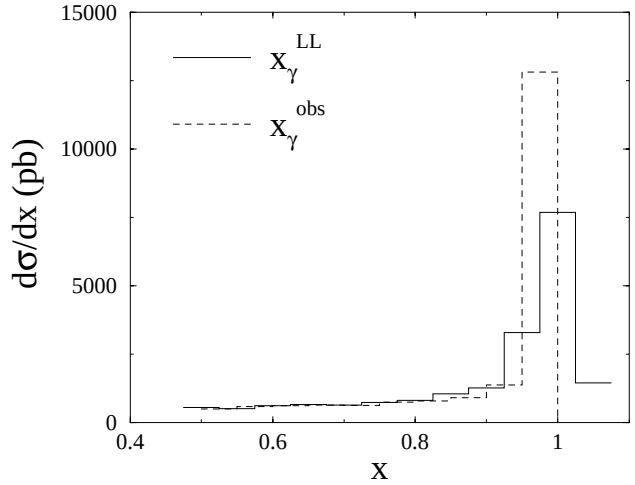

Fig. 2. A comparison between the distributions $d\sigma/dx_\gamma^{LL}$ and $d\sigma/dx_\gamma^{obs}$, with the following cuts on the two high E_T jets: $E_T^{leading} > 12\ GeV$ and $E_T^{trailing} > 10\ GeV$ and $0 < \eta < 1$, and the k_T-algorithm for the definition of jets

to 1.0, the two distributions are very similar [1]. (The AFG [17] and ABFOW [18] distributions with $N_f = 4$ have been used for this calculation). Currently experimentalists integrate x_γ^{obs} over the range $.75 \leq x_\gamma^{obs} \leq 1$. Therefore the singular behaviour of the cross section is smoothed and should not forbid the phenonemological application of NLL calculations.

We can also see from Fig. 2 how much NLL corrections modify the x_γ distribution which is proportional to $\delta(1 - x_\gamma)$ at the LL accuracy. NLL corrections generate terms with x_γ^{obs} or x_γ^{LL} different from 1 and the simple picture of a photon directly interacting with a quark of the hard subprocess at $x_\gamma = 1$ is lost. But one must also keep in mind that the separation of the cross section $d\sigma/dx_\gamma^{obs}$ into a direct part and a resolved part is factorization scheme dependent and that $d\sigma^{direct}/dx_\gamma^{obs}$ has no physical sense on its own (the same remark is valid for x_γ^{LL}).

To study this problem we computed the observable $d\sigma/dx_\gamma^{LL}$ in two factorization schemes, the so-called DIS_γ and $\overline{MS}$ ones. For the resolved part, we used for the former case the GRV distributions of quarks inside the photon and for the latter the AFG distributions. (Here we also use the ABFOW proton distributions). We can see that both the direct and resolved part are very different in these two schemes (Fig. 3), but that this difference is much smaller for the total cross section which is factorization scheme independent. The remaining difference partly comes from different hadronic inputs in the two sets of distributions.

We now turn to the study of the gluon contents of the photon and to the possibility of constraining it through the observation of the distribution $d\sigma/dx_\gamma^{obs}$. The sensitivity of $d\sigma/dx_\gamma^{obs}$ to the gluon distribution does not only depend on the value of x_γ^{obs}, but also on the various kinematical cuts imposed on the 2-jet phase space. Clearly the region of positive and large rapidities corresponds to small values of x_γ^{obs} and to an enhancement of $d\sigma/dx_\gamma^{obs}$. This is verified in Fig. 4. We divided the rapidity range in the lab frame for the two leading jets in subintervals: $0 < \eta < 1$ and $1 < \eta < 2$. We have also used asymmetric cuts on the transverse momenta, as it is done by experimental collaborations, in order to avoid the instabilities which appear when these momenta become close to each other. Then in each of these rapidity intervals we compared the x_γ^{obs} distribution obtained with the AFG photon density with cross-sections for which we have artificially reduced and increased the gluon distribution by 30%. We found that the influence of the gluon increases with the rapidities and in fact the differences between these three curves become sizeable only when $1 < \eta < 2$. Indeed an increase of 30% of the gluon density results in an increase of approximately 25% for the cross-section around $x_\gamma^{obs} = 0.2$. Therefore a determination of the gluon contents of the photon would require to use such cuts on rapidities. Such a study would be able to test the gluon density $F_\gamma^g(x)$ in the region $x \approx 0.2$ where it is very poorly known.

5 Comparison with H1 and ZEUS data

In this section we analyse recent H1 and ZEUS data to assess the possibility to put constraints on the gluon distributions in the photon and in the proton. With this intention we investigate the sensitivity of various cross sections to changes in the gluon distributions, and we compare their variations to the experimental errors. In this way we obtained an estimate of the accuracy with which gluon distributions can be extracted from present data, and from future high statistics experiments. We modify the gluon distributions by increasing or decreasing their normalizations by a few tens of percents. This method has the advantage of leaving unchanged the well-determined quark distributions and to quantify the gluon modifications in a simple way. Of course gluon distributions are constrained by other experiments. But, as discussed in the introduction, the gluon in the photon is not well constrained by DIS $\gamma\gamma^*$ data. As for the gluon in the proton we are going to study observables sensitive to the distribution at small $x \approx 0.02$. In this region the gluon is pinpointed by the slope of F_2 and it was shown by the CTEQ collaboration that a variation of about $\pm 10\%$ of F_p^g in this region and at a scale of 100 GeV would cause clear disagreements with DIS plus Drell-Yan data [26]. However this conclusion was not obtained by performing an error analysis but only by tuning gluon parametrisation, which might artificially reduce the range of variation by being too restrictive. A more recent study obtained a gluon density 30% bigger than CTEQ4M about $x \approx 0.02$ and at a scale of 20 GeV [27]. Errors on the gluon determination are also presented in [19]. Thus we think that it is interesting to find how

[1] Note that the shape of the cross sections around $x_\gamma = 1$ depends on the width of the x_γ-bin, because the Born and virtual contributions are proportional to $\delta(1 - x_\gamma)$. If the width is too small, the cross section may even be negative (the positive real contributions do not compensate anymore the negative virtual contributions)

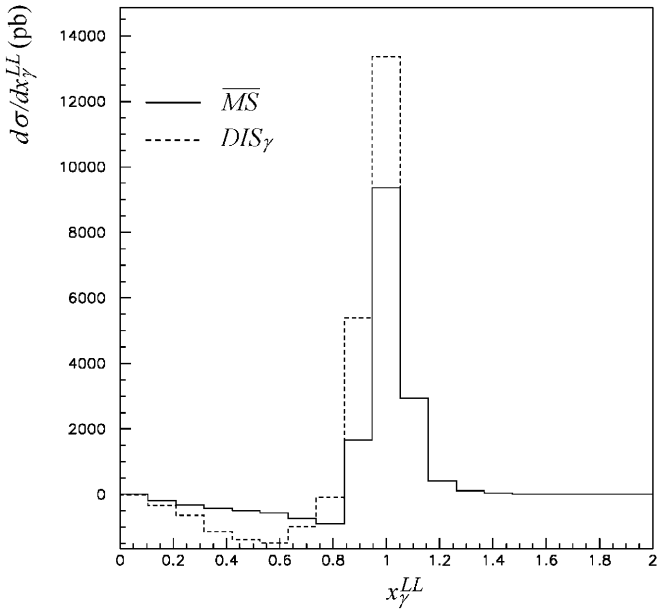

a Direct contribution

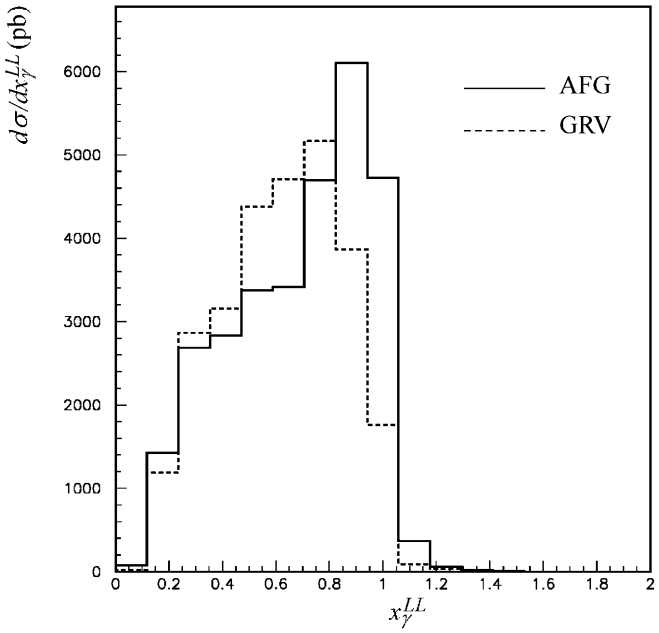

b Resolved contribution

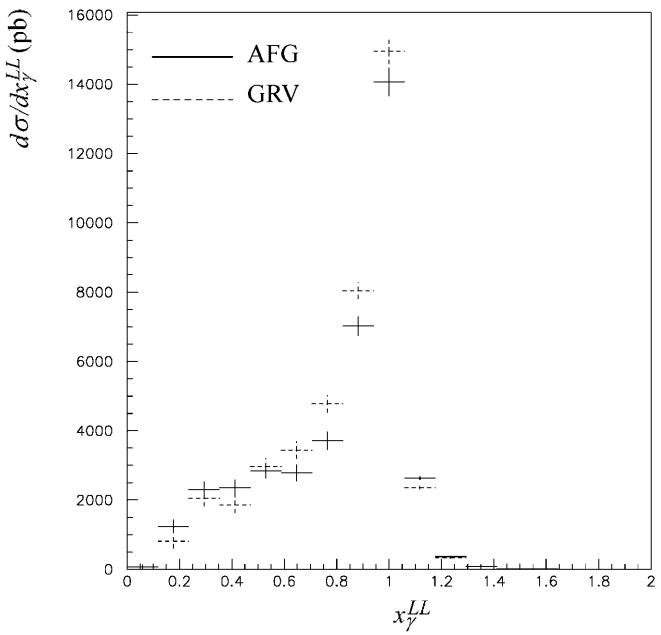

c Total contribution

Fig. 3a–c. Distribution $d\sigma/dx_\gamma^{LL}$ for the direct, resolved and total contributions with the AFG ($\overline{MS}$ scheme) and GRV (DIS_γ scheme) photon density as well as ABFOW proton density, with the following cuts on the two high E_T jets: $E_T > 9.2\ GeV$ and $-1 < \eta < 2$, and using a cone algorithm with $R = 1$ and no R_{sep} to define the jets

much photoproduction can constrain this density in this x-range.

The interested reader may find more global comparisons between theory and data in [20,22,23]. The inputs we use in this section have been defined in Sect. 3 where we computed single-jet cross sections. More details on the kinematical parameters used for dijet cross sections are given below[2].

[2] To follow H1 and ZEUS conventions, we call jet 1 and jet 2 the jets with the highest energies; we used the labels 3 and 4 in the preceeding sections

The ZEUS collaboration presents cross sections which depend on the jet transverse momenta, or on the jet rapidities [23]. Therefore we do not have a direct access to $d\sigma/dx_\gamma^{obs}$, however we can study data corresponding to regions of the jet phase space in which the role of the gluon in the photon or that of the gluon in the proton is enhanced. These regions are essentially defined by large or small values of the jet rapidities: large rapidities correspond to small x_γ and small rapidities to small x_p (see the LL expressions for x_p and x_e below formula (2)).

Let us start with the case of large jet rapidities. Experiment and theory are compared in Fig. 5. The dijet cross

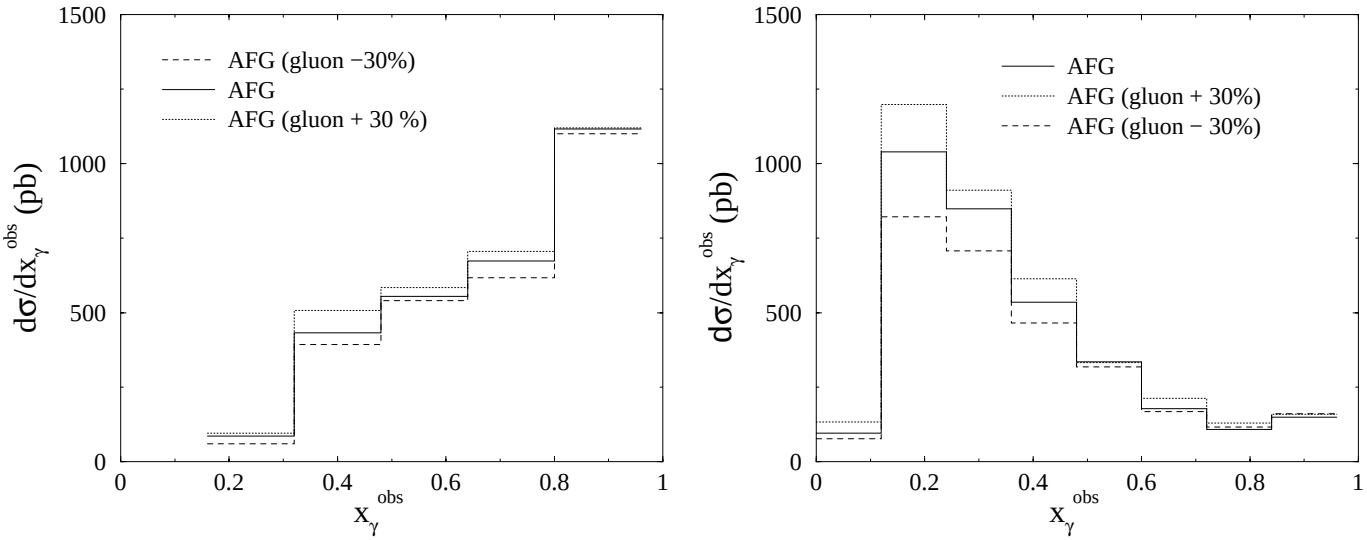

a $0 < \eta < 1$ **b** $1 < \eta < 2$

Fig. 4a,b. Cross sections $d\sigma/dx_\gamma^{obs}$ with the following cuts for the two high E_T jets: $E_T^{leading} > 12\ GeV$ and $E_T^{trailing} > 10\ GeV$ and 2 different cuts on their rapidities, and using the k_T-algorithm to define the jets. Curves with the gluon distribution varied by ±30% around the AFG one are also displayed

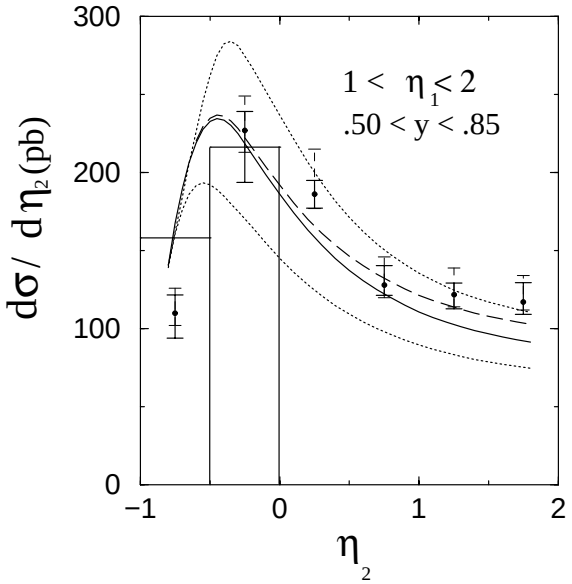

Fig. 5. The cross section $d\sigma/d\eta_2$ compared with ZEUS data [23]. (Full error bars: statistical errors; dashed error bars: systematic errors including energy-calibration errors). Full line: $.5 \leq y \leq .85$. Dotted lines: $.45 \leq y \leq .85$ (upper) and $.55 \leq y \leq .85$ (lower). The dashed line is obtained with the distribution g/γ increased by 20%

sections in this figure correspond to events with at least one jet with transverse energy larger than 14 GeV, the transverse energy of the other jet being larger than 11 GeV; it is integrated over $1 < \eta_1 \leq 2$. The real photon kinematical domain is specified by $Q^2_{max} = 1$ GeV^2 and $.5 < y < .85$ (cf expression (1)). The jets are defined with the k_T-algorithm [15] and the scales M and μ are set equal to the transverse energy of the most energetic jet.

To test the sensitivity of $d\sigma/d\eta_2$ to the gluon density in the photon, we increased the gluon distribution uniformly by a factor of 1.2. Comparing the full and dashed curves, we see that this factor produces an increase of the cross section for large values of η_2 by some 10%. As expected the backward region, corresponding to large values of x_γ, is not affected; the gluon distribution in the photon decreases much faster than the quark distributions. In this region $d\sigma/d\eta_2$ rapidly varies with η_2 and better comparison with data is obtained by integrating $d\sigma/d\eta_2$ in the experimental bins. This has been done for the two bins: $-1. \leq \eta_2 \leq -.5$ and $-.5 \leq \eta_2 \leq .0$. The agreement between theory and data is quite good in the second bin but the data at larger η_2 favor a larger gluon distribution in the proton. But one must notice that the present experimental errors are larger than the effect produced by an increase of the gluon distribution by 20%. In the backward region, a clear discrepancy appears which could be attributed to hadronization effects as discussed in [24].

It is also worth again noting the great sensitivity of the cross section to the y-range of the photon. The energy of the incoming photon is reconstructed from the final hadron energies with the Jacquet-Blondel method. Various corrections have to be applied to this "photon energy" y_{JB} in order to obtain the true photon energy y [25]. In Fig. 5 we show the effect of a 10% error on the determination of the lower bound of the y variable. It is very large for negative values of η_2. Even in the forward region, this 10% error produces an effect much larger than the 20% variation of the gluon distribution. Actually this "error" is included in the discussion of the systematic errors quoted in [25]. But because the dispersion of y_{JB} around y may reach 10%, a better theoretical prediction could be obtained by taking into account the dispersion of the upper and lower bounds of the variable y.

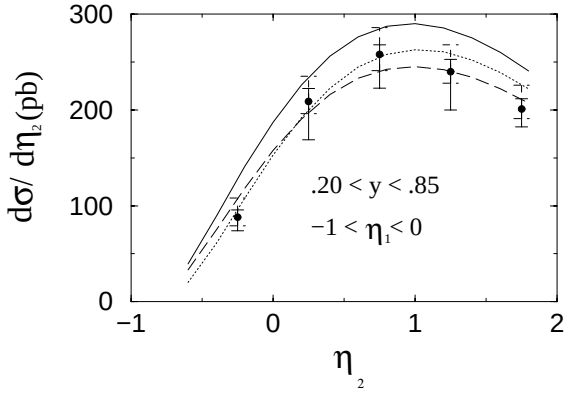

Fig. 6. The cross section $d\sigma/\eta_2$ compared with ZEUS data [23]. (Full error bars: statistical errors; dashed error bars: systematic errors including energy-calibration errors). Full line: $.2 \leq y \leq .85$. Dotted line: $.2 \leq y \leq .80$. The dashed line is obtained by reducing the distribution g/P by 20%

In Fig. 6 we present the results of a similar study done for negative values of η_1. In this kinematical range, we can infer from Fig. 6 that the cross section depends very little on moderate changes of the gluon distribution in the photon. Therefore this kinematical range is well-suited for a study of the gluon in the proton at $x_p \sim 2E_T/2E_p \sim 15/880 = .018$. Here we choose data corresponding to the following y-range: $.2 < y < .85$. Also displayed are predictions obtained for $.2 \leq y \leq .8$, and those obtained with a gluon distribution in the proton multiplied by a factor .8. We see that a small modification of the y-range produces an effect similar to a change of the gluon distribution by 20%. Here again, the experimental errors are larger than the effects due to a modification of the theoretical inputs, but there is a slight indication that data prefer a smaller gluon distribution in the proton.

Finally we turn to the E_T-spectrum obtained by the ZEUS collaboration. Here again we choose to study the large rapidity region with the dijet cross section integrated over the ranges $1 \leq \eta_1 \leq 2$ and $1 \leq \eta_2 \leq 2$:

$$d\sigma/dE_T^{leading} = \int_1^2 d\eta_1 \int_1^2 d\eta_2 \; \frac{d\sigma}{dE_T^{leading}\; d\eta_1\; d\eta_2} \quad (8)$$

$E_T^{leading}$ is the transverse energy of the leading jet (highest E_T). The transverse energy of the other jet is constrained by the condition 11 GeV $< E_T < E_T^{leading}$. Our results are shown in Fig. 7. Predictions for the range $.25 \leq y \leq .85$ and for a gluon in the photon increased by 20% are also shown. A slightly better agreement with data is obtained in the latter case (hardly distinguishable on a logarithmic plot).

The H1 collaboration presented results [20] under a form which is very close to the one advocated in the preceding section; the authors chose to give the cross section $d\sigma/(dx_\gamma^{obs} d\ \mathrm{Log}((E_T^{jets})^2/\mathrm{GeV}^2))$ with the definitions

$$E_T^{jets} = \frac{E_{T1} + E_{T2}}{2} \quad (9)$$

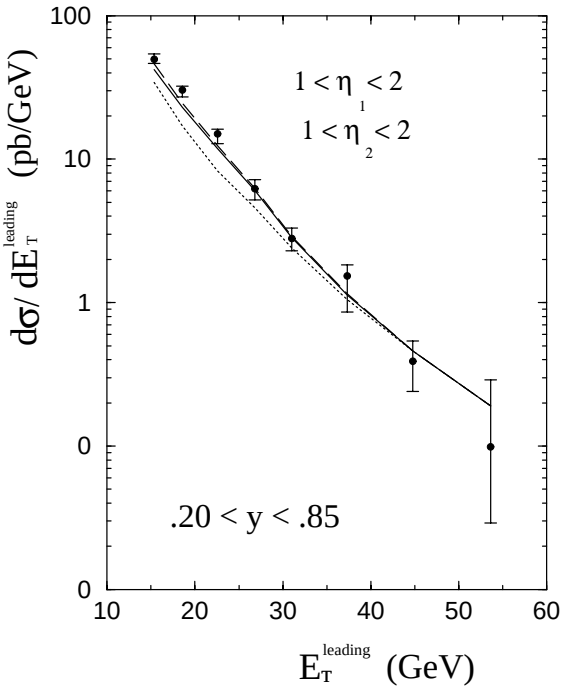

Fig. 7. The cross section $d\sigma/dE_T^{leading}$ compared to ZEUS data [23]. (In this figure the energy-calibration errors are not included in the error bars). Full line: $.20 \leq y \leq .85$. Dotted line: $.25 \leq y \leq .85$. The dashed line is obtained by increasing the gluon distribution g/γ by 20%

where E_{T1} and E_{T2} are the transverse energies of the two jets with the highest transverse energies in an event. Other kinematical requirements are

$$\begin{aligned} \frac{|E_{T1} - E_{T2}|}{2E_T^{jets}} &< .25 \\ 0 < \frac{\eta_1 + \eta_2}{2} &< 2 \\ |\eta_1 - \eta_2| &< 1 \quad . \end{aligned} \quad (10)$$

The cuts on the "real" photon variables are $Q^2_{max} = 4\ \mathrm{GeV}^2$ and $.2 < y < .83$. We use a cone algorithm [21] with $R = .7$ and no R_{sep} in agreement with [20]. Moreover we avoid double counting of jet configurations by choosing the jet of highest E_T (made of two partons) when the parton configuration also allows to construct two jets (made of one parton each). The scales M and μ are set equal to E_T^{jets}.

In Fig. 8 we compare our results with H1 data in the range $2.30 < \mathrm{Log}\left(\frac{E_T^{jets}}{GeV}\right)^2 \leq 2.50$ where E_T^{jets} is large enough to allow us to neglect (in a first approximation) hadronisation effects and underlying event contributions. A good agreement[3] is obtained with data, except for x_γ^{obs}

[3] Unlike other observables, here we disagree with the predictions of [22]. Our values are higher at small x_γ^{obs}, by a few tens of percents; this cannot be explained by the different values of N_f used in the calculations (4 flavors in [22] and 5 in this paper)

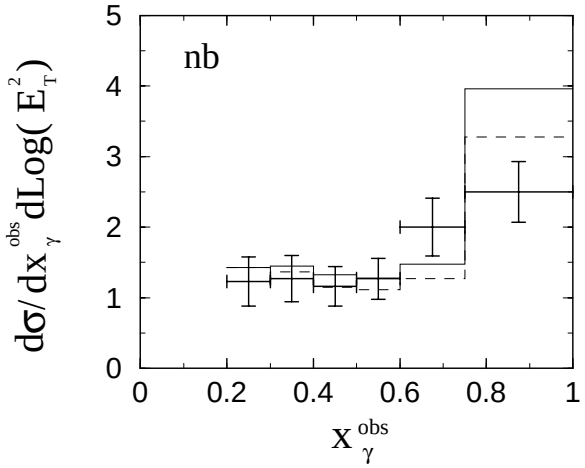

Fig. 8. The cross section $d\sigma/(dx_\gamma^{obs} d\mathrm{Log}((E_T^{jet}/\mathrm{GeV})^2))$ in the range $2.3 \leq \mathrm{Log}(E_T^{jet}/\mathrm{GeV})^2 \leq 2.5$ [20]. Full curve: $.2 \leq y \leq .83$; dashed curve: $.25 \leq y \leq .83$

close to one (the "Direct" domain) where theory overshoots data. It must be again noted that the theoretical curve is very sensitive to the photon energy range $y = E_\gamma/E_e$. A change of the lower limit from $y = .20$ to $y = .25$ leads to the dashed line in Fig. 8; the cross section decreases for $x_\gamma^{obs} \simeq 1.0$. However it is unlikely that the disagreement for $x_\gamma^{ob} \sim 1$ between theory and H1 data could be explained by a dispersion of the upper and low bounds in y. (The variation of y_{low} by 25% studied above is certainly bigger than the experimental systematic error). A decrease of the gluon distribution in the proton would decrease $d\sigma/dx_\gamma^{obs}$ in all bins in x_γ^{obs}. It is compatible with data at low x_γ^{obs}, but its effect at large x_γ^{obs} is not sufficient to put theory in agreement with data. The resolved contribution is also important in the highest x_γ^{obs}-bin, a kinematical region which explores the quark contents of the photon at large x_γ. In this domain the quark distribution is given by the pointlike component (non pointlike contributions of the "Vector Meson Dominance" type are negligible) which cannot be modified in an arbitrary way, and adjusted to data. For instance the difference between the AFG and GRV parametrization is small in this region (see Fig. 3).

The first conclusion that we can draw from this study of H1 and ZEUS data is that overall there is a good agreement between experiment and theory. However the systematic errors are non-negligible and correspond roughly to variations of the theoretical predictions coming from modifications by ± 20% of the gluon distribution normalizations. Therefore it appears difficult to constrain the gluon distributions with an accuracy better than a few tens of per cents with the present data.

Part of the errors should cancel in the ratio

$$dN/dx_\gamma^{obs} = \frac{d\sigma/dx_\gamma^{obs}}{\int_0^1 dx_\gamma^{obs}\ d\sigma/dx_\gamma^{obs}} \qquad (11)$$

which could allow a better determination of the x shape of the distributions functions. However we would thus loose any information on the absolute normalization.

6 Conclusions

In this paper we described a new NLL event generator for photoproduction reactions involving the direct and resolved contributions, and we used it to assess the possibility to measure the quark and gluon contents of the photon from photoproduction experiments. (Actually we assumed that the quark distributions in the photon were fixed from $\gamma\gamma^*$ DIS experiments and we concentrated on the gluon contents).

The cross section $d\sigma/d\bar{x}_\gamma$, where $\bar{x}_\gamma$ is related to the scaled momentum x_γ of partons in the photon, is quite appropriate to a study of these contents. We discussed two definitions of $\bar{x}_\gamma$: $\bar{x}_\gamma = x_\gamma^{obs}$, the well-known definition of the ZEUS collaboration, and $\bar{x}_\gamma = x_\gamma^{LL}$, a variable which reduces problems of infrared sensitivity. Then we showed that the cross section $d\sigma/dx_\gamma^{obs}$ is sensitive to the gluon density of the photon only if we require the two jets with the highest transverse energy to have positive rapidities.

A relatively good agreement between theory and experiment is found when confronting the predictions, obtained with the CTEQ4M and GRV distributions, with H1 and ZEUS data. It is interesting to note that H1 and ZEUS data are compatible with a 20% increase of the gluon contents of the photon (Fig. 6, $\eta_1 \sim 1.5$, Fig. 8, $E_T^{leading} \sim 20$ GeV) and with a 20% decrease of the gluon contents of the proton (Fig. 5, $x_\gamma^{obs} \sim 1$ where the direct contribution is important; Fig. 7). Unfortunately this remark cannot be made more quantitative, because the systematic errors, essentially coming from the uncertainties in the measurement of the jet energies, are large and of the same order as the variations of the theoretical predictions due to gluon distribution modifications. One must also keep in mind the great sensitivity of the cross section to the photon energy-range. The knowledge of the resolution of the variable y (obtained from the Jacquet-Blondel variable y_{JB}) should allow a more accurate prediction. However it is interesting to remark that 1996 and 1997 preliminary ZEUS data [25] also favor a larger gluon distribution in the photon.

Until now we have not discussed the theoretical uncertainties coming from the scale dependence of the cross sections. These uncertainties were carefully studied in [9] and in [22], and found to be of the order of a few tens of percents for large variations of the values of the factorization and renormalization scales. In this paper we continue this study by looking at the sensitivity of the cross section $d\sigma/(dx_\gamma^{obs} d\mathrm{Log}(E_T^{jets})^2)$ which can be compared with H1 data (Fig. 5); we make this study for the range $.75 \leq x_\gamma^{obs} \leq 1$ and with the kinematical conditions of Fig. 5. The scales are $M = \mu = \kappa E_T^{jets}$ and κ is varied between .5 and 2. Our results are summarized in Table 1.

We note that the cross section $d\sigma/dx_\gamma^{obs}$ is quite stable and varies by less than 5% when the scales $M^2 = \mu^2$ vary

Table 1. The sensitivity of the direct and resolved photoproduction cross-sections to the renormalization and factorization scale $M = \mu = \kappa \cdot E_T^{jets}$ (normalized to the total contribution at $\kappa = 1.0$)

κ	**Direct contribution**	**Resolved contribution**	**Total contribution**
0.5	0.634	0.384	1.018
0.75	0.578	0.432	1.010
1.00	0.547	0.453	1.000
1.50	0.512	0.474	0.986
2.00	0.491	0.482	0.973

by a factor 16. The theoretical errors appear to be well under control, at least for this observable.

So we can conclude that, in the future, the possibility to accurately determine the gluon distribution in the photon relies on the possibility to improve the experimental systematic errors. In the future also statistics will be larger and higher E_T regions will be accessible. The corresponding data will put more constraints on the parton distributions.

Acknowledgements. We would like to thank Joost Vossebeld for an interesting correspondence on ZEUS results.

References

1. P. Chiappetta, R. Fergani and J. Ph. Guillet, Z. Phys. **C69** (1996) 443
2. P. Aurenche, L. Bourhis, M. Fontannaz, J. Ph. Guillet, Proceedings of the Workshop "Future Physics at HERA", 570 (1996)
3. R.K. Ellis and J.C. Sexton, Nucl. Phys **B269** (1986) 445
4. B. W. Char et al., Maple V Language Reference Manual, Springer Verlag
5. A new version of the Multidimensional Integration and Event Generation Package, BASES/SPRING, S. Kawabata, National Laboratory for High Energy Physics, Tsukuba
6. HBOOK Reference Manual, Applications Software Group, Computing and Network Division, CERN
7. B. W. Harris and J. F. Owens, Phys. Rev. **D56** (1997) 4007
8. M. Klasen and G. Kramer, Z. für Physics **C76** (1997) 67
9. S. Frixione and G. Ridolfi, Nucl. Phys. **B507** (1997) 315
10. S. Frixione, Z. Kunszt, A. Signers, Nucl. Phys. **B467** (1996) 399
11. P. Aurenche, M. Fontannaz and J. Ph. Guillet, Phys. Lett. **B338** (1994) 98. It should be noticed that the resolved contribution shown in this paper is too high by a factor 2. This has been corrected for the actual comparison
12. ZEUS collaboration, presentation at the XXIX ICHEP, Vancouver, July 1998
13. CTEQ collaboration, H. L. Lai et al., Phys. Rev. **D55** (1997) 1280
14. M. Glück, E. Reya, A. Vogt, Phys. Rev. **D46** (1992) 1973
15. S. Catani, Y. L. Dokshitzer, M. H. Seymour, B. R. Webber, Nucl. Phys. **B406** (1993) 187
16. M. Derrick et al., ZEUS collaboration, Phys. Lett. **B348** (1995) 665
17. P. Aurenche, M. Fontannaz, J. Ph. Guillet, Z. Phys. **C64** (1994) 621
18. P. Aurenche et al., Phys. Rev. **D39** (1989) 3275
19. T. Carli, Nucl. Phys. B, Proc. Supplement **79** (1999) 18
20. H1 collaboration, C. Adloff et al., Eur. Phys. J. **C1** (1998) 97
21. J. E. Huth et al., Proceedings of the 1990 DPF Summer Study on High Energy Physics, Snowmass, Colorado, E. L. Berger Ed. S. D. Ellis, Z. Kunszt, D. E. Soper, Phys. Rev. Lett. **69** (1992) 3615
22. M. Klasen, T. Kleinwort and G. Kramer, Eur. Phys. J. **C1** (1998) 1
23. ZEUS collaboration, J. Breitweg et al., Eur. Phys. J. **C11** (1999) 35
24. B. W. Harris, M. Klasen and J. Vossebeld, Proceedings of the workshop "Monte Carlo Generators for HERA Physics" (Hamburg 1998/1999), hep-ph 9905348
25. Dijet photoproduction at High Transverse Energies, PhD thesis, Joost Vossebeld, Amsterdam University, September 1999
26. J. Huston et al., Phys. Rev. **D58** (1998) 114
27. V.Barone et al., Eur. Phys. J. **C12** (2000) 243